Strong impact of separatrix conditions on full-radius L-mode predictive integrated modelling [1]

B. Liu[1,*], C. Bourdelle[2], S. Wiesen[1], F. Casson[3], T. Fonghetti[2], M. J. Pueschel[1,4,5], N. Rivals[2], E. Vergnaud[2], and and the WEST team[6]

[1]*Dutch Institute for Fundamental Energy Research, 5612 AJ Eindhoven, The Netherlands*
[2]*CEA, IRFM, F-13108 Saint-Paul-lez-Durance, France*
[3]*UKAEA, Abingdon, Oxfordshire OX14 3DB, United Kingdom*
[4]*Eindhoven University of Technology, 5600 MB Eindhoven, The Netherlands*
[5]*Department of Physics and Astronomy, Ruhr University Bochum, D-44780 Bochum, Germany*
[6]*The WEST Team (*`http://west.cea.fr/WESTteam`*)*
[*]*Corresponding author: b.liu@differ.nl*

1 Introduction

The separatrix parameters play an important role in determining the core plasma performance. The operational limits such as disruptive L-mode density limit and L-H transition, are evaluated with the participation of separatrix density $n_{e,sep}$ and temperature $T_{e,sep}$ [2]. The separatrix operational space (SepOS) is derived on the ASDEX Upgrade, which has subsequently been extended to C-Mod and applied to predictive studies for devices such as SPARC [3]. Consistently, multi-machine database studies on devices such as JET, ASDEX Upgrade and WEST report sensitivities of density peaking, transport and global confinement to edge conditions [4]. Experiments and modellings on ASDEX Upgrade and C-Mod have shown that variations of separatrix conditions can induce a rapid core plasma response by modifying the turbulent transport [5, 6]. These considerations motivate a dedicated study of the impacts of separatrix conditions on turbulent transport and full-radius core profiles.

The present work builds on the High-Fidelity Pulse Simulator (HFPS), a Python workflow based on the JINTRAC/JETTO suite of codes, coupled to the Integrated Modelling and Analysis Suite (IMAS) [2, 7]. A schematic overview of the HFPS workflow is shown in Fig. 1. In this framework, JETTO solves the transport partial differential equations for temperatures and density up to the separatrix. The neutral fueling is calculated with FRANTIC, while ESCO is used for the magnetic equilibrium. Transport coefficients consist of neoclassical and turbulent contributions, computed with NCLASS and TGLF-sat2, respectively.

In this work, the HFPS settings are based on the WEST L-mode discharge #57757, which is a lower single-null scenario sustained for about 100 s, with $\langle n_e \rangle_{line} \approx 3.0 \times 10^{19}\,\mathrm{m}^{-3}$, $P_{LHCD} = 3\,\mathrm{MW}$. Good agreements between HFPS simulation and experimental diagnostics have been reported for plasma profiles, energy confinement time and loop voltage [8]. As shown by the blue line in Fig. 2, the reference calculation starts at 84.5 s up to 87.5 s, which covers about 600 energy confinement time τ_E ($\sim 0.06\,\mathrm{s}$). The separatrix electron density and temperature are fixed to $1.1 \times 10^{19}\,\mathrm{m}^{-3}$ and 72.3 eV, and the separatrix ion temperature is same as electron value. Nitrogen is considered as the external impurity species. The recycling coefficient is set to 0.9, the gas puffing flux is $6.0 \times 10^{20}\,\mathrm{s}^{-1}$ and the neutral energy is 10 eV. To keep the gas puffing flux constant, the feedback control on $\langle n_e \rangle_{line}$ is deactivated in the reference case.

Similar to the workflow in [6], the impacts of separatrix conditions on core profiles and transport are investigated. Plasma current, density and temperature are predictively calculated,

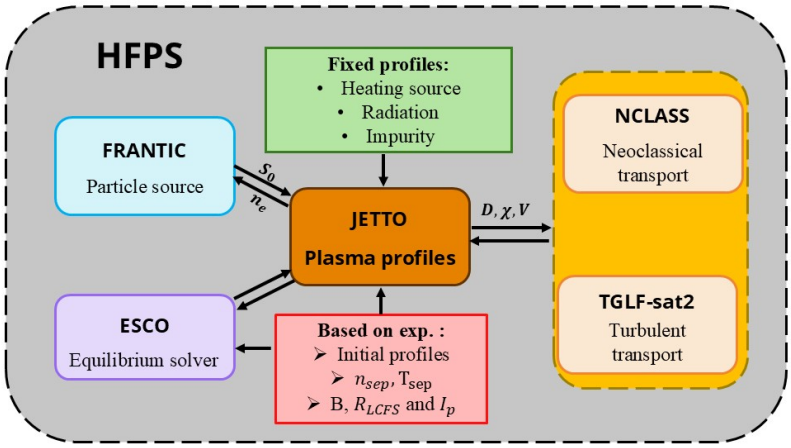

Figure 1: Schematic of the HFPS workflow used in this work, showing the coupling of JETTO with FRANTIC, ESCO, NCLASS and TGLF-sat2 for self-consistent core plasma simulations.

while heating source and radiation profiles are frozen. This setup allows the response of the core plasma to separatrix boundary conditions to be isolated within a controlled integrated modelling framework.

2 Impacts of separatrix conditions on core transport and profiles

2.1 HFPS simulation results

Fig. 2 illustrates the core plasma response to $n_{e,sep}$. With $n_{e,sep}$ is increased to three and five times the reference value, the electron density rises over the whole radius and develops a steeper profile up to $\rho \approx 0.6$. With the fixed heating source, the higher electron density and resulting stronger electron–ion equipartition at higher collisionality lead to reduced electron temperature. The energy content W_{th} increases with $n_{e,sep}$ due to more particle numbers even though the electron temperature is reduced. Consistent with the stronger density peaking obtained at higher $n_{e,sep}$, the effective transport coefficients decrease. By contrast, the neutral source profiles in the edge region ($0.8 \leq \rho \leq 1.0$) show modest changes compared with the large variations in density.

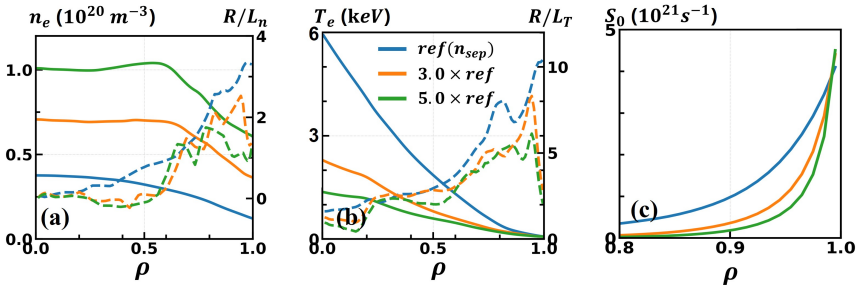

Figure 2: HFPS sensitivity scan in $n_{e,sep}$: (a) electron density profiles and normalized density gradients; (b) electron temperature profiles and normalized temperature gradients; (c) neutral particle source.

The parameter scan of $T_{e,sep}$ shows that increased $T_{e,sep}$ leads to reduced electron density and raised temperature. Beyond the free explorations of $n_{e,sep}$ and $T_{e,sep}$, more physical separatrix conditions are obtained from the SOLEDGE simulations and empirical scaling laws derived from WEST C4 campaigns database analyses. Overall, compared with the relatively modest variations in the neutral particle source profiles, the response of the effective transport is significantly stronger,

which indicates that the profile modification is mainly transport-driven rather than source-driven. Similar results have also been reported by the ASTRA modelling of ASDEX Upgrade L-mode discharge, where the role of boundary conditions was explored in the absence of particle sources [6].

In order to identify the dominant driving parameters of transport dependence on separatrix conditions, the effective particle diffusion D_{eff} is compared with collisionality ν^* and normalized gradients $R/L_n, R/L_T$. A clear trend is found that higher ν^* is generally associated with lower D_{eff} across different radial positions and boundary-condition cases. In contrast, the correlations between D_{eff} and $R/L_n, R/L_T$ are weaker and more scattered. These results suggest that collisionality is the main parameter linking separatrix-condition variations to the modified turbulent particle transport in HFPS.

2.2 Turbulent transport analysis by TGLF-sat2

Additional checks of computed V_{pol} and E_r do not support neoclassical contributions as the primary explanation for the observed transport trend. Standalone TGLF-sat2 calculations are therefore employed to investigate the instability regime and to quantify the sensitivity of the dominant modes to collisionality and other local parameters.

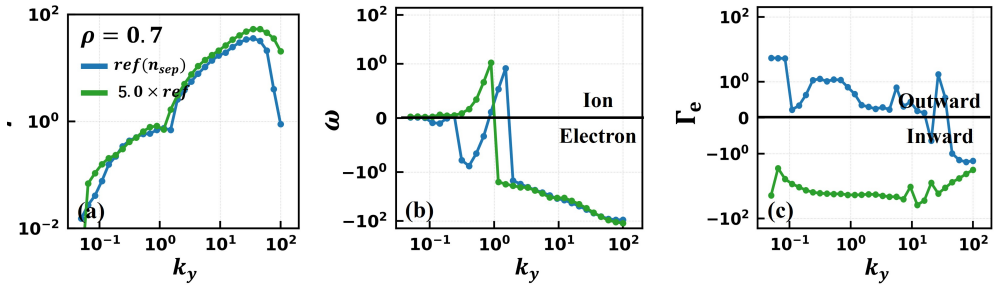

Figure 3: Linear TGLF-sat2 spectra at $\rho = 0.7$ for the reference (blue) and high-density ($5.0\times ref$, green) cases.

The spectrum of the reference case at $\rho = 0.7$ exhibits both ion-propagating and electron-propagating branches. The particle flux is predominantly outward and the heat flux is mainly contributed by electrons. It indicates a mixed regime with a significant TEM-like contribution. As the $n_{e,sep}$ increasing, the dominant instability shifts to ion propagation, and ion heat flux becomes the leading contribution, which corresponds to ITG mode characteristics. At electron scales, both cases show electron-propagating modes with small ion heat-flux fraction. This is an ETG instability characteristic, which is weakly affected by the $n_{e,sep}$ scan. A dedicated collisionality scan at $k_y = 0.2$ confirms this interpretation: increasing collisionality reduces the growth rate, shifts the frequency from the electron to the ion diamagnetic direction, and reverses the electron particle flux from outward to inward. Therefore, the collisionality rising with higher separatrix density shifts the edge turbulence from a TEM-dominated regime with outward particle transport towards an ITG-dominated regime with inward particle transport.

Similar analysises at $\rho = 0.5$ and $\rho = 0.9$ provide additional support for the key role of collisionality. At $\rho = 0.5$, increasing collisionality drives a transition from electron- to ion-diamagnetic propagation in the reference case, accompanied by a reversal of the particle flux from outward to inward and an increased ion heat-flux fraction. The high-density case is already mainly ion-propagating and is less sensitive to collisionality, indicating more ion-dominated transport. At $\rho = 0.9$, increasing collisionality first suppresses the electron-branch contribution and reduces

outward particle transport, while at higher collisionality a resistive or DTEM-like response may emerge.

2.3 Thought experiments within HFPS

The effective particle and energy confinement times are estimated from a numerical free decay of the core plasma. As shown in Fig. 4, starting from steady HFPS states, heating and particle sources are switched off, while the separatrix density and temperatures are reduced to a small positive floor for numerical stability. The subsequent decay of $\langle n_e \rangle_{vol}$ and W_{th} is fitted with exponential functions to obtain particle and energy confinement times τ_p and τ_E. The results show that both τ_p and τ_E increase with $n_{e,sep}$, with a stronger dependence for τ_E. Over the explored range, τ_E follows approximately $\tau_E \propto n_{e,sep}^{0.58\pm0.18}$. Thus, increasing separatrix density not only raises the core density and energy, but also enhances the effective energy confinement in the present HFPS simulations.

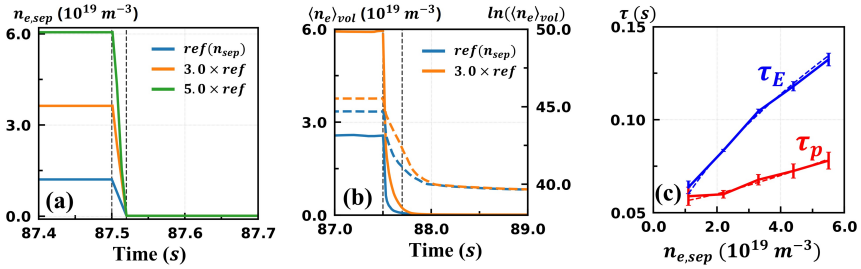

Figure 4: Method to estimate confinement times. Time evolution of (a) separatrix density $n_{e,sep}$, (b) volume-average density $\langle n_e \rangle_{vol}$ (solid lines) and $ln(\langle n_e \rangle_{vol})$ (dashed lines), (c) effective particle and energy confinement times.

3 Conclusions

Full-radius HFPS simulations of a WEST L-mode discharge show a strong sensitivity of core density to the separatrix conditions, due to the modified transport. Increasing separatrix density leads to higher density peaking up to $\rho = 0.6$, with reduced electron temperature and enhanced energy content. In particular, increasing separatrix density by a factor of five results in a 35% increase in energy content, despite fixed heating and particle sources. This trend is opposite to the experimental database correlation, where larger $n_{e,sep}$ is associated with lower energy content, indicating that additional coupled experimental effects remain to be understood. Conversely, increasing separatrix temperature reduces core density while raising temperature.

Correlation and TGLF-SAT2 analyses identify collisionality as the key parameter: higher collisionality reduces effective particle diffusion, shifts the dominant ion-scale response from TEM-like towards ITG-like characteristics, and promotes inward particle transport. Controlled thought experiments further show that higher $n_{e,sep}$ increases both particle and energy confinement times. Future work will extend this analysis to broader WEST datasets and other devices.

References

[1] Liu B 2025 submitted to Nuclear Fusion.
[2] Bourdelle C 2025 Plasma Phys. Control. Fusion 67 043001.
[3] Eich T et al 2025 Nuclear Materials and Energy 42 101896.
[4] Bourdelle C 2023 Nuclear Fusion 63 056021.
[5] Rodriguez-Fernandez P 2018 Phys. Rev. Lett. 120 075001.
[6] Bonanomi N et al 2025 Plasma Phys. Control. Fusion 67 065028.
[7] Wiesen S et al 2017 Nuclear Fusion 57 076020.
[8] Fonghetti T et al 2025 Nuclear Fusion 65 056018.